THE SCS-CN MODEL AND ITS APPLICATION

Edward Ching-Ruey, LUO 羅 慶 瑞

Associate Professor of Department of Civil Engineering, National Chi-Nan University, Taiwan

中華民國水利技師公會全國聯合會　理事

*Author for Correspondence: edward.luo@msa.hinet.net

ABSTRACT

River catchments exhibit spatial variability of landscape characteristics such as geology, topography, soils, land use and vegetation. These characteristics govern the partitioning of precipitation into runoff and evapotranspiration and contribute to defining the spatial distribution of soil moisture within the catchment. Soil moisture patterns, in turn, are a key factor in influencing runoff generation and the hydrological response of a catchment. This interaction of soil moisture and hydrological processes as a function of landscape variability affects both vertical and lateral water fluxes. Vertical fluxes occur by processes such as infiltration, percolation and evapotranspiration. Lateral fluxes are related to redistribution processes of surface runoff, water in the saturated and unsaturated soil zone or in the groundwater flowing roughly parallel to the terrain surface. In hydrological models it is required to account for the spatial variability of landscape characteristics and for the processes as those mentioned above if the hydrological response of a catchment should be adequately represented. Several approaches have been taken to incorporate landscape variability into hydrological models. In this paper, we will deeply consider and analyze the main factors in SCS-CN model and present its application with some discussion.

Key Words: SCS-CN; Hydro-Morphodynamic Parameters; Sensitivity Analyses; Concentration Time;Lag Time; Roughness; Precipitation; Runoff; Evaporation; transpiration;

INTRODUCTION

Surface runoff can be estimated directly from conceptual models such as the runoff curve number (RCN) method or indirectly from physically based infiltration models such as the Green–Ampt method (Ponce, 1989; McCuen, 2003; Mishra and Singh, 2003). Both methods are widely accepted models for predicting surface runoff in both agricultural and urbanized watersheds due to their simplicity and to the limited number of parameters required for runoff prediction. In addition, they have been integrated into many hydrologic, storm water

management and water quality models such as the erosion productivity impact calculator EPIC (Sharpley and Williams, 1990), the soil and water assessment tool SWAT (Arnold et al.,1998), and the storm-water management model SWMM (Rossman et al., 2003). The key parameters involved in the RCN and the Green–Ampt methods are the runoff curve number (CN) and the saturated hydraulic conductivity (Ksat) respectively, which can be obtained from tables as functions of soil texture, management practice, and land use. The use of singular tabulated CN and Ksat values without verification can result in large errors in predicting surface runoff. With different chosen soils to estimate the CN and Ksat values.in situ runoff from rainfall simulators was quite necessary.

The model approach used to determine the runoff volume was the SCS-CN method (SCS, 1972). With this method, the precipitation excess is a function of cumulative precipitation, soil type, land use/cover and antecedent moisture. Considering the initial loss and the potential maximum retention, the precipitation excess can be calculated; the maximum retention and the basin characteristics are related through the curve number. The standard SCS curve number method is based on the following relationship between rainfall depth, P, and runoff depth, Q (USDA, 1986; Schulze et al., 1992).

In many runoff–infiltration assessment studies, the methods commonly used are the rational method, Curve Number (CN) method, Horton's model for infiltration capacity and the Green Ampt infiltration model (Thomas, 2001). The Rational method is one of the simplest and widely used methods commonly applied in urban hydrology in order to calculate peak runoff in small urban catchments. The Horton infiltration method appears simple but its application require field measurements of infiltration rate and parameters of this method cannot be estimated from soil and land cover. The Green Ampt model is an accurate physically based model for determining infiltration, but it has parameters to be measured in field and the input data needed for the implementation of model is hard to determine. Many models developed or used to estimate runoff are based on Curve Number, which is an empirical parameter used in hydrology for predicting direct surface runoff or infiltration from rainfall excess (USDA-SCS, 1993). The curve number method was developed in the 1950s by the United States Department of Agriculture (USDA) Natural Resources Conservation Service (NRCS), which was formerly called the Soil Conservation Service or SCS and is described in NRCS's National Engineering Handbook, Section 4 (USDA-SCS, 1993). Although the CN method is designed for a single storm event, it can be scaled to find average annual runoff values (Ma, 2004). This method is also described in most engineering hydrology textbooks, and it was thoroughly reviewed by Ponce and Hawkins (1996). Many of the hydrologic models meant to estimate non-point source pollution and assess water quality in catchments

have implemented the SCS Curve Number method to estimate surface runoff.

The tern 'Runoff' refers to the portion of rainfall that makes its way to stream channels, lakes, or oceans as surface runoff (also called direct surface runoff) and/or subsurface runoff which comes in the form of interflow, through flow, return flow and base flow from groundwater storage. Here only the surface runoff flow is dealt with. Surface runoff will only occur when the rate of precipitation exceeds the rate of water infiltration into the soil. The amount of rainwater that runs off during/immediately after a rainfall event depends heavily on the amount of rainfall, initial abstraction (i.e., initial loss due to interception, evaporation, depression and detention storage), and the type and hydrologic condition of the ground it lands on i.e., infiltration characteristics of the soil, soil moisture, antecedent rainfall, impervious surface etc. (Thomas, 2001). Following a rainfall event, the rainfall reaching the surface after the initial abstraction translates into infiltration, surface runoff, interflow and base flow.

Soil surface roughness affects surface depression storage, water infiltration, overland flow velocity as well as overland flow organization. Few studies exist on the relationship between roughness and the infiltration characteristics of a tilled surface, although this may be more important. Four types of roughness:(1) micro-relief variations, which are due to individual grains or micro-aggregates, (2) random roughness, which is related to soil clodiness, (3) oriented roughness, which describes the systematic variations in topography due to farm implements and (4) higher order roughness, representing elevation variations at the field, basin or landscape level. Studies on roughness and its effects on arable land usually concentrate on random and oriented roughness because these roughness types are far more important than micro-relief variations while higher order roughness is adequately described by conventional topographical surveys. Both oriented and random soil roughness affect various hydrologic and erosion processes on arable land. Soil roughness determines the storage of water on the soil surface and may indirectly influence its infiltration capacity. The velocity of overland flow is controlled by the hydraulic resistance of the soil surface. Soil roughness affects the organization of the drainage pattern on the field and the catchment scale, which in turn may have important implications for the spatial distribution of sediment sources and sinks. Conversely, some of these processes affect surface roughness. Many authors have studied the effect of rainfall on Random Roughness (RR) and developed models to describe the decrease in RR as a function of amount of rainfall or rainfall kinetic energy. Surface roughness data have been used to calculate surface storage capacity, i.e. the maximum equivalent water depth that can be stored on the soil surface. Various algorithms have been used to calculate depression storage. In general, these algorithms try to determine the amount

of water needed to fill all the depressions present on the surface up to their "pour point", i.e. the water level at the moment that they start to overflow. However, the results of the calculations depend on the algorithm used to delineate depressions as well as on the assumptions made with respect to open depressions, i.e. depressions connected to the plot border.

THEORETICAL CONSIDERATION

To determine how the runoff is distributed over time we must introduce a time-dependent factor. The time-of concentration (Tc) is used in the SCS methods. The Tc is most often defined as the time required for a particle of water to travel from the most hydrological remote point in the basin to the point of collection. There are several methods available for calculating Tc, one of them is the SCS Lag Method:

$$T_L = 0.6 T_c$$
$$T_L = L^{0.8}[(1000/CN) - 9]^{0.7}/1900 S_0^{0.5}$$
$$Y = (25400/CN) - 254$$

where TC is the time of concentration (minutes); TL is the watershed lag time (minutes); L is the length of longest watercourse (ft); S_0 is the mean slope of the basin (%); and CN is the curve number. Y is maximum storage depth (mm).

It is important to note that surface runoff and infiltration in any location can be estimated through the following equation:

Surface Runoff = Rainfall – Initial abstraction – Infiltration ....(1)

The SCS-CN method employs the water balance equation and two fundamental hypotheses. The water balance is expressed as:

$$P = I_a + F + Q \quad \text{...(2)}$$

The first hypothesis states that the ratio of direct runoff to potential maximum runoff is equal to the ratio of infiltration to potential maximum retention and, according to the second hypothesis, the initial abstraction is some fraction of the potential maximum retention. These are respectively expressed as:

$$\frac{Q}{P - I_a} = \frac{F}{S} \quad \text{...(3)}$$

and

$$I_a = \lambda S \quad \text{..(4)}$$

where P = total precipitation (mm), I_a = initial abstraction (mm), F= accumulative infiltration (mm), Q= direct runoff (mm), S= potential maximum retention (mm), λ = initial abstraction coefficient (vary from 0 to ∞, while 0.2, a standard value), λ =0.05 has been advocated for field use. The SCS-CN method was formed with the combination with Eqs. (2) and (3) as the following expression:

$$Q = \frac{(P-I_a)^2}{P-I_a+S} = \frac{(P-\lambda S)^2}{P+(1-\lambda)S} \quad\quad\quad\quad (5)$$

Here $P \geqq I_a$, Q=0 otherwise. The SCS-CN parameter S can be determined as Eq (6) with λ =0.2:

$$S = 5[(P + 2Q) - \sqrt{Q(4Q + 5P)}] \quad\quad\quad\quad (6)$$

S can be transformed to CN scale using the following empirical relation:

$$CN = \frac{25400}{S+254} \quad\quad\quad\quad (7)$$

where S is in mm and CN is a non-dimensional parameter.

The above SCS-CN methodology was developed for small ungauged agricultural watersheds and suggested the methodology to be suitable for area less than $250 km^2$.

Estimation of potential evapotranspiration (PET) is required for water availability computations; estimation of daily, weekly, and monthly flows for multipurpose reservoir operation; scheduling of irrigation projects; preparation of long-term flow forecasts; and many other aspects of water resources planning and management. In general, ET is the second largest component of the catchment water balance and the PET data forma the key input to the rainfall-run off model. PET can be estimated using energy balance, mass transfer, combination of energy balance and mass transfer based empirical and semi-empirical approaches. The water balance method yields the best estimates of mean long-term evaporation from large (plain) river basin. The estimation of ET using soil water balance method is however often limited due to inconvenience and inaccuracy in measurement of ground water inflow and outflow. Nevertheless, for the reasons of computational simplicity, stability, ease in understanding and grasping, the soil-water balance method is still frequently used in rainfall-runoff modeling. The proportionality concept of the popular SCS-CN method is employed in the simple water balance equation to derive a relationship between CN and mean PET using the usually available long-term daily rainfall-runoff data. To show the existence of a relationship between CN and ET, it is in order to consider all the factors

governing CN and evaluate the impact of their variation on ET. Here, it is worth emphasizing that, since PET represents the maximum rate at which water is transferred to atmosphere, all the factors responsible to ET also affect PET of a watershed.

The term initial abstraction I_a in SCS-CN methodology consists of interception, surface detention, evaporation and infiltration (before the time to ponding after which runoff begins). The water that contributes to interception and surface detention and storage is evaporated back to the atmosphere and contributes neither to runoff nor to infiltration. The infiltrated water before the time to ponding may be interpreted as to have satisfied the atmospheric demand of water absorption (molecular adsorption in particular) of the soil air column, similar to evaporation. Therefore, the water held by interception, surface detention, and infiltration at the beginning of a storm finally goes back to atmosphere through evapotranspiration. Thus, I_a depends on ET. As I_a increases, direct runoff Q decreases or, in turn, S increases or CN decreases. Thus ET and CN are inversely related. Active leaf area that actively contributes to transfer of surface heat and vapor. Since biological processes are carried out by the leaves, LAI (leaf area index) is fully responsible for energy, water, and gas exchange between the soil/plant to the atmosphere. Normally LAI increases with growing period and it reaches maximum before harvesting or at flowering. LAI varies greatly among species and within species due to differences in site, age, stand composition, density, and season. Species growing in cool and arid climates usually have small LAI and reach maximum LAI at later stage than those growing in warm and wet environments. Since surface resistance and LAI are inversely related, all the factors governing LAI affect surface resistance, and hence, ET.

From Eq. (3) as Q→(P-I_a), F→S. Since I_a= 0.2S, the maximum water loss =1.2S. In terms of antecedent moisture condition (AMC) of fully dry condition, it is equal to 1.2SI, where the subscript I refers to AMCI. Since, by definition, PET corresponds to unlimited amount of moisture supply to vegetation, as described above, the assumption in the proposed PET computation is that the rainfall (P) is always greater than or equal to 1.2SI during the storm duration. Here, it is worth emphasizing that I_a accounts for all those initial water losses, such as interception, evaporation, surface detention, and infiltration, describable in terms of evaporation and not available for either plant use or runoff generation. The water that can transpire through vegetation during the storm duration can be equal to SI, if the moisture is fully available. Thus, the sum of I_a and S for AMC I describe the potential amount of evapotranspiration that can occur in a watershed during the storm period. Thus, there appears to be a relation existing between PET and SI, which can be described in power form as:

$$PET = \alpha S_I^\beta \quad \text{... (8a)}$$

Eq.(7a) can be more generalized as:

$$ET = \alpha S^{\beta} \quad \text{...(8b)}$$

where α and β are greater than 0, and we can see that higher S generating larger ET with lower CN in Eq. (7).

The soil moisture W and evapotranspiration E are important and given as:

$$E_T + E_S = \beta_{T,S}\left(E^* - E_I\right) \quad \text{...(9a)}$$

$$\beta_{T,S} = \frac{W}{W^*} \quad \text{...(9b)}$$

$$E = E_I + E_T + E_S \quad \text{..(9c)}$$

where ET is the daily transpiration (moisture transferred from the soil to the atmosphere through the root-stem-leaf system of vegetation); ES is the daily soil evaporation (moisture transferred from the soil to the atmosphere by hydraulic diffusion through the pores of the soil); EI is the daily interception loss (water evaporated from the wet surface of the vegetation and wet surface of the soil) during rain storm; $\beta_{T,S}$ is the coefficient of transpiration plus soil evaporation, taken as a function of soil wetness; E* is the daily potential evapotranspiration; W is the root-zone moisture at the end of the day; and W* is the root-zone storage capacity.

From Eqs. (9a) & (9c),

$$\beta_{T,S} = \frac{E - E_I}{E^* - E_I} \quad \text{..(10)}$$

Coupling of Eqs. (9b) and (10) leads to

$$\frac{E - E_I}{E^* - E_I} = \frac{W}{W^*} \quad \text{...(11)}$$

The ratio of of F (=W) to S (=W*). Thus, Eq.(11) states that, similar to the SCS-CN proportionality hypothesis ((Eq.(3)), the ratio of actual evapotranspiration to the potential evapotranspiration is equal to the ratio of actual infiltration (or moisture retention) to the potential maximum retention. A substitution of Eq. (3) into Eq.(11):

$$\frac{E - E_I}{E^* - E_I} = \frac{F}{S} = \frac{Q}{P - I_a} \quad \text{..(12)}$$

When further coupled with Eq.(5), Eq.(12) yields the following:

$$E = E_I + \frac{(P - I_a)(E^* - E_I)}{P - I_a + S} \quad \text{..................................(13)}$$

Here, EI, by definition, represents the daily interception loss (water evaporated from the wet surface of the vegetation and wet surface of the soil) during the rain storm. It is however a representation of the above described SCS-CN initial abstraction (I_a) that includes not only interception losses but also surface detention, initial infiltration, and evaporation. Thus, within the frame-work of SCS-CN terminology, EI can be taken as I_a. Therefore, Eq.(13) can be recast as:

$$E = I_a + \frac{(P - I_a)(E^* - I_a)}{P - I_a + S}$$ ....(14)

In addition, since parameter λ in Eq. (6), is a regional parameter that depends on geological and climatic

factors and hence an important parameter in PET estimation, results may be improved with the use of a value other than the standard value of 0.2. Furthermore, it is possible to quantitatively examine the impact of climate change on hydrological system on employing CN-PET relationship.

The estimation of root-zone soil moisture

It was derived from a simplified soil water balance equation for semiarid environments that provides a closed form of the relationship between the root zone and the surface soil moisture with a limited number of physically consistent parameters. d the use of an exponential filter of the form exp(−t/T), where T is the characteristic length time or recession constant. This filter was used to convert the time series of surface measurements to a signal that is able to capture the dynamics of the lower soil layer. The great advantage of this filter lies in its simplicity due to the fact that it makes use of one parameter only. Moreover, the derived soil moisture index (SWI) relies only on the surface observation (remotely sensed data). Therefore, this approach, which from now on will be referred to as the SWI method, has been tested with both simulated and measured data, providing good results, and has been extensively used to improve the description of the root-zone soil moisture in rainfall–runoff applications (Manfreda et al., 2011; Brocca et al., 2010, 2012; Matgen et al., 2012a). The growing interest in this approach makes it critical to provide a physical interpretation of the parameter T that is influenced by a number of physical processes controlling soil moisture fluctuations. T represents the parameter of the exponential autocorrelation function of soil moisture. For this reason, T is influenced by all the physical processes affecting the temporal fluctuations of soil moisture (e.g. evapotranspiration, soil hydraulic properties, soil depth, number of soil layers, etc.). In this way, they demonstrated that the parameter T is proportional to the ratio between the soil water content at field capacity and potential evapotranspiration.

The most relevant water mass exchange between the two layers is represented by infiltration. Other processes such as lateral flow and capillary rise are assumed negligible with respect to infiltration. The challenge is to define a soil water balance equation where the infiltration term is not expressed as a function of rainfall, but of the soil moisture content in the surface soil layer. This may allow the derivation of a function of the soil moisture in one layer as a function of the other one. The water flux from the top layer can be considered significant only when the soil moisture exceeds field capacity. Assuming that the soil moisture movement from the upper to the lower layer during a rainfall event can be modelled following the Green–Ampt approach (Green and Ampt, 1911), one can assume that all water in the first layer above field capacity will move into the lower layer within one day. One may immediately realize that the equation contains only one parameter that is represented by T = nZr/C, named the characteristic time length. C is a pseudo-diffusivity coefficient, n is the soil porosity of the given layer, and Zr [L] is the depth of the corresponding layer that depends on the soil properties. Under such assumptions, the infiltration flux from the top layer to the lower occurs instantaneously and is described by:

$$n_1 Zr_1 y(t) = n_1 Zr_1 y[s_1(t), t]$$
$$= n_1 Zr_1 \begin{cases} (s_1(t) - s_{c1}), & s_1(t) \geq s_{c1} \\ 0, & s_1(t) < s_{c1} \end{cases} \quad\text{...(15)}$$

y(t) is fraction of soil saturation infiltrating in the lower layer, n1 is the soil porosity of the first layer, Zr1 [L] is the depth of the first layer, s1 (θ1/n1) is the relative saturation of the first layer (given by the ratio between the soil water content, θ1, and the porosity, n1, of the first layer), and sc1 is the value of relative saturation at field capacity of the first layer of soil. The above equation implies the assumption of an infinite permeability of the soil when the relative saturation reaches any value above field capacity. It is also necessary that the first layer not be infinitesimal, because this condition will lead to zero infiltration. Moreover, the model does not account for the saturation effect of the lower layer. It is necessary to note that, in order to avoid undesired underestimation of the infiltration, the surface soil moisture value should be referred to the first 5–10 cm of soil. A thickness of less than 5 cm may lead to numerical problems in this and other hydrological models. For this reason, we assumed that the soil losses decrease linearly from a maximum value under well-watered conditions to 0 at the wilting point.

Defining x2 = (s2 − sw2)/ (1 − sw2) as the "effective" relative soil saturation of the second soil layer and w0 =(1 − sw2)n2Zr2 the soil water storage, the soil water balance can be described by the following expression:

$$(1 - s_{w2})n_2 Zr_2 \frac{dx_2(t)}{dt} = n_1 Zr_1 y(t) - V_2 x_2(t),$$

....(16)

where s2 represents the relative saturation of the soil, sw2 is the relative saturation at the wilting point, n2 is the soil porosity, Zr2 [L] is the soil depth, V2 [L/T] is the soil water loss coefficient accounting for both evapotranspiration and percolation losses, and x2 is the "effective" relative soil saturation of the second soil layer. It should be noted that this equation does not account for the high non-linearity that characterizes the soil loss function for high values of soil moisture. This simplification, along with the fact that the infiltration does not account for the saturation effect, implies some limitations in the use of such an approach in humid environments. The model in fact was thought mainly for a semiarid-environments with flat surfaces and neglecting the presence of phreatic surfaces, effects due to topographic convergence (e.g. subsurface flows), the presence of frozen soils, etc. The equation above can be simplified using normalized coefficients as:

$$a = \frac{V_2}{(1 - s_{w2})n_2 Zr_2}, \quad b = \frac{n_1 Zr_1}{(1 - s_{w2})n_2 Zr_2}.$$

....(17)

The value of these parameters can be related directly to the ratio of the depths of the two layers and the soil water loss coefficient. As a consequence, the soil water balance equation becomes:

$$\frac{dx_2(t)}{dt} = b\, y(t) - a\, x_2(t).$$

....(18)

Assuming an initial condition for the relative saturation x2(t) equal to zero, one may derive an analytical solution to this linear differential equation:

$$x_2(t) = \int_0^t b\, e^{a(w-t)} y(w) dw.$$

....(19)

For practical applications, one may need the discrete form as well:

$$x_2(t_j) = \sum_{i=0}^{j} b\, e^{a(t_i - t_j)} y(t_i) \Delta t.$$

....(20)

Substituting $\Delta t = t_j - t_{(j-1)}$, , one may derive the following expression for the soil moisture in the second layer based on the time series of surface soil moisture:

$$x_2(t_j) = x_2(t_{j-1}) e^{-a\,(t_j - t_{j-1})} + b\, y(t_j)(t_j - t_{j-1}).$$

....(21)

that may be rewritten as a function of s2 as:

$$s_2(t_j) = s_{w2} + (s_2(t_{j-1}) - s_{w2}) e^{-a(t_j - t_{j-1})} + (1 - s_{w2}) b\, y(t_j)(t_j - t_{j-1}).$$ ....(22)

The four parameters sw2, sc1, a, and b. may be estimated from the soil texture, the soil depth, and the soil water losses. The parameter a is a function of potential evapotranspiration and soil permeability that can be estimated using regression functions. It should be noted that the result may produce values higher than 1 and that these are automatically set equal to 1. In particular, the soil porosity (n), the bubbling pressure head (ψ), and the soil permeability at saturation (Ks) were taken from Rawls et al. (1993), while the values of sw and sc have been calculated adopting the Brooks and Corey (1964) model ($\psi(s) = \psi_s S^{-1/m}$, where m is the pore-size index.

Modeling daily reference evapotranspiration (ET0) and ET

Estimation of reference evapotranspiration (ET0) is needed to support irrigation design and scheduling,and watershed hydrology studies. There are many available methods to estimate evapotranspiration from a water surface, comprising both direct and indirect methods. The general equations for estimating ET0 are:

1. Penman-Monteith method (FAO56),

$$ET_0 = \frac{0.408\Delta(R_n - G) + \gamma\left(\frac{900}{T+273}\right)U_2(e_a - e_d)}{\Delta + \gamma(1 + 0.34U_2)}$$ ....(23)

where ET0 = reference evapotranspiration (mm /day); D = slope of the saturation vapor pressure function (kPa /℃); G is soil heat flux density (MJ/m^2 day); Rn = net radiation (MJ/m^2 day); c = psychometric constant (kPa/℃); T = mean air temperature (℃); U2 = average 24 h wind speed at 2 m height (m /sec); ea is the saturation vapor pressure (kPa); ed is the actual vapor pressure (kPa), and ea - ed is the saturation vapor pressure deficit (kPa). The various terms presented in the above equation was computed on a daily basis and the ET0 was estimated as per procedure outlined in FAO-56 (Allen et al.1998).

2. Hargreaves–Samani method,

$$ET_0 = 0.0023\, R_a \left(\frac{T_{\max} + T_{\min}}{2} + 17.8\right) \sqrt{T_{\max} - T_{\min}}$$ ....(24)

where Tmax is daily maximum air temperature (℃), Tmin is daily minimum air temperature (℃), and Ra is extra-terrestrial radiation, which is defined as the solar radiation received at the top of the earth's atmosphere on a horizontal surface.

3. Priestley and Taylor method,

$$ET_0 = \frac{\alpha}{\lambda} \frac{\Delta}{\Delta + \gamma} (R_n - G)$$ ....(25)

where $\alpha = 1.26$; λ = the latent heat of the evaporation (MJ /kg); D is the slope of the saturation vapor pressure function (kPa /℃); G is the soil heat flux density(MJ/m^2day); Rn = net radiation (MJ/ m^2day);

c = the psychometric constant (kPa/℃).

Various daily climatic data, that is, daily mean relative humidity, sunshine duration, maximum, minimum and mean air temperature, and wind speed are used as inputs to estimate the ET0. The performances of the models are evaluated using root mean square errors (RMSE), mean absolute error (MAE), Willmott index of agreement (d) and correlation coefficient (CC) statistics:

$$CC = \frac{\frac{1}{N}\sum (O_i - O_m)(P_i - P_m)}{\sqrt{\frac{1}{N}\sum_{i=1}^{n} (O_i - O_m)^2}\sqrt{\frac{1}{N}\sum_{i=1}^{n} (P_i - P_m)^2}}$$ ....(26)

$$RMSE = \sqrt{\left|\frac{1}{N}\sum_{i=1}^{N} (O_i - P_i)^2\right|}$$ ....(27)

$$MAE = \frac{1}{N}\sum_{i=1}^{N} |O_i - P_i|$$ ....(28)

$$d = 1 - \frac{\sum_{i=1}^{N} (P_i - O_i)}{\sum_{i=1}^{N} (|P_i - O_m| + |O_i - O_m|)^2}$$ ....(29)

Here N is the number of data points, Oi is some measured value, and Pi is the corresponding model prediction. Om and Pm are the average values of Oi and Pi. The Willmott index of agreement (d) is an indicator of model performance. It carries a value from 0 to 1 where the index of 1 indicates perfect agreement.

Monitoring of regional evapotranspiration (ET) allows decision makers to (1) follow where, when, and how much water has moved into the atmosphere by ET; (2) monitor crop performance and the effects of drought for famine prediction; (3) better evaluate the performance of irrigation systems; (4) improve estimates by distributed hydrologic and weather models; and (5) estimate root zone soil moisture conditions.

We compute the latent heat flux as the residual of the surface energy balance:

$$\lambda E = R_n - G - H$$ ....(30)

where Rn is net radiation, G the soil heat flux, H the sensible heat flux, and λE is the latent heat flux. By use of an internal calibration of the energy balance the incorporates effects of regional advection of energy and dry air, via the employment of the Penman-Monteith equation can substantially increase ET from irrigated agriculture and riparian vegetation in semiarid and arid climates. When soil moisture in the root zone decreases and soil resistance to water movement increases, the net effect is a reduction in actual ET (λE). When the soil is wet, most of the available energy (net radiation, Rn, minus soil heat flux, G) is used for ET (latent heat flux) and almost no energy is left for sensible heat flux (H). When the soil is dry, most of the available energy is used to heat soil and air and latent heat flux (ET) is small. One way to express this partitioning of radiant energy is the evaporative fraction (Λ) that is defined as:

$$\Lambda = \frac{\lambda E}{\lambda E + H} = \frac{\lambda E}{R_{\mathrm{n}} - G} \dots\dots\dots\dots\dots\dots\dots\dots\dots\dots\dots\dots\dots\dots\dots\dots\dots\dots\dots(31)$$

The energy partitioning calculated with the evaporative fraction is primarily related to the amount of vegetation and soil moisture content. The following equation was using in situ root zone soil moisture measurements:

$$S = \frac{\theta}{\theta_{\mathrm{sat}}} = e^{\frac{\Lambda-1}{0.42}} \dots\dots\dots\dots\dots\dots\dots\dots\dots\dots\dots\dots\dots\dots\dots\dots\dots\dots\dots(32)$$

where S is degree of saturation (0.0-1.0), θ is volumetric water content, and θ sat is volumetric water content at saturation. Eq. (32) was derived from soil moisture measurements obtained on grass land on alluvial soils and loess, as well as from rainfall (vineyard, barley, wheat) and irrigated crops (maize, alfalfa). Another issue with constructing continuous series of ET with satellite imagery is the large temporal variability of ET fluxes. The daily ET can vary by a factor 2 or 3 from one day to another depending on weather conditions, especially cloudiness. As the ET observed from space on image days is often not representative of ET values on non-image days, direct insertion of ET fluxes into hydrologic models can cause substantial error. Instead, more robust variables with less temporal variability such as the ETrF or root zone soil moisture (S or θ) are preferred for insertion into hydrologic decision support tools and for time-integration of ET between satellite overpass dates. The ETrF is calculated for each pixel of an image as:

$$\mathrm{ET_r F} = \frac{\mathrm{ET}}{\mathrm{ET_r}} \dots\dots\dots\dots\dots\dots\dots\dots\dots\dots\dots\dots\dots\dots\dots\dots\dots\dots\dots (33)$$

where ET is the actual estimated ET for each pixel, and ETr is the standardized reference ET for a tall crop. The ETrF is similar to the crop coefficient (Kc) that is defined as:

$$K_{\mathrm{c}} = \frac{\mathrm{ET}_{\mathrm{c}}}{\mathrm{ET}_{\mathrm{ref}}}$$ .... (34)

where ETc is the crop ET under standard conditions and ETref is the (generic) reference ET.

Root zone soil moisture is another robust hydrologic variable that is correlated with daily ET but without its large temporal variability. Root zone soil moisture is an important tool for the incorporation of variable ET fluxes into hydrologic models when no high-quality hourly weather data are available to calculate ETr.

In the actual ET, the potential evapotranspiration (PET), and volumetric soil water content are related as follows:

$$\mathrm{ET} = \mathrm{PET}\left(\frac{\theta - \theta_{\mathrm{wp}}}{0.75\left(\theta_{\mathrm{sat}} - \theta_{\mathrm{wp}}\right)}\right)$$ ....(35)

where θ is the volumetric soil water content, θ wp is the wilting point, and θ sat is the saturated volumetric soil water content. If $\theta > 0.75\,\theta$ sat, the ET is considered equal to the PET. PET is considered equal to the reference ET for a tall crop (ETr) that is calculated from the meteorological data measured at a ground-based station.

The governing factors on roughness, n

The efficiency of various roughness indices for the prediction of depression storage. When comparing existing indices, the best results were obtained with a combination of the Limiting Difference index and slope: combinations of Random Roughness and slope also gave reasonable results.

Soil roughness does not only affect the runoff amount through depression storage, but may also affect the volume and rate of infiltration. Several experimental studies have shown an effect of surface roughness on infiltration rate. On rough surfaces the amount (or kinetic energy) of rainfall required to initiate runoff is higher. This is not only due to larger depression storage, but also to the fact that the process of surface sealing is affected by surface roughness. It was observed that surface sealing was reduced on rough surfaces. This could be explained by the fact that rough surfaces have a larger surface area, which means that the impact force of raindrops is spread over a larger area. In addition, the local slope of the surface will be higher on rough surfaces, which leads to a lower impact force in the direction normal to the soil surface. Thus, the initial roughness of the surface appears to have a strong control on runoff and infiltration during the first phases of the crusting process. Infiltration rates of surfaces with a fully developed crust are more or less independent of initial soil roughness.

Variations in infiltration capacity on natural surfaces can occur at various scales due to variations in soil thickness, vegetation, etc. If variations in infiltration capacity are important enough, this automatically implies that the average infiltration capacity of the soil surface under rainfall will increase with rainfall intensity. In some cases, part of this variation could be related to variations in mic-topography whereby the soil mounds below grass tussocks has a much higher infiltration capacity than the lower-lying non-vegetated areas. Consequently, an increase of surface water depth led to a strong increase in infiltration as increasingly more permeable areas of the soil surface became submerged. The observed spatial variability in crust properties (related to soil roughness) leads to an increase of the apparent infiltration capacity of the surface with increasing ponding depth. The effect of water depth on infiltration appeared to be far more important for a well-aggregated soil than for a strongly crusting soil. The observed variations are such that they may have a very significant influence on the total runoff production of a field.

Several available equations to predict values of n for rivers can be found and categorized as: (A) equations that are based on bed sediment size; (B) equations that are based on the ratio of flow depth or hydraulic radius over sediment size; and (C) equations that includes water-surface slope besides bed sediment size and hydraulic radius or flow depth. In the present study, seven equations were evaluated as follows:

Table 1 Suggested Manning *n* for natural streams (Chow, 1959).

Type of channel and description	Minimum	Normal	Maximum
Stream on plain			
Clean, straight, full stage, no rifts or deep pools	0.025	0.030	0.033
Same as above, but more stones and weeds	0.030	0.035	0.040
Clean, winding, some pools and shoals	0.033	0.040	0.045
Same as above, but more stones and weeds	0.035	0.045	0.050
Clean, winding, some pools and shoals, weeds and more stones	0.045	0.050	0.060

(A) equations that are based on bed sediment size:

$$\text{Strickler (1923): } n = \frac{1}{21.1}d_{50}^{1/6} \quad\text{...(36).}$$

$$\text{Meyer-Peter \& Muller (1948): } n = \frac{1}{26}d_{90}^{1/6} \quad\text{...(37)}$$

$$\text{Lane \& Carlson (1953): } n = \frac{1}{21.14}d_{75}^{1/6} \quad\text{..(38)}$$

(B) equations that are based on the ratio of flow depth or hydraulic radius over sediment size:

$$\text{Limerinos (1970): } n = \frac{0.113R^{1/6}}{0.35 + 2.0\log_{10}\left(\frac{R}{d_{50}}\right)} \quad \dots\dots\dots\dots\dots\dots\dots\dots\dots(39)$$

$$\text{Bray (1979): } n = \frac{0.113y_o^{1/6}}{1.09 + 2.2\log_{10}\left(\frac{y_o}{d_{50}}\right)} \dots\dots\dots\dots\dots\dots\dots\dots\dots(40)$$

(C) equations that includes water-surface slope besides bed sediment size and hydraulic radius or flow depth:

$$\text{Brownlie (1983): } n = \left[1.893\left(\frac{R}{d_{50}}\right)^{0.1374} \times S^{0.1112}\right]$$
$$\times 0.034 \times (d_{50})^{0.167} \quad \dots\dots\dots\dots\dots\dots\dots(41)$$

$$\text{Bruschin (1985): } n = \frac{d_{50}^{1/6}}{12.38} \times \left(\frac{R}{d_{50}} \times S_o\right)^{1/7.3} \quad \dots\dots\dots\dots\dots\dots\dots(42)$$

There is one important question that whether the value n is constant or not, we have explained as:

$$\bar{U}/u_* = 6.25 + 5.75\log(R/k_s)\text{for fully roughly} \quad k_s = f(d_m)\dots\dots\dots\dots(43)$$
$$\bar{U}/u_* = 6.25 + 5.75\log(Ru_*/v) \text{ for fully smoothly}\dots\dots\dots\dots\dots(44)$$
$$\bar{U} = (1/n)R^{2/3}S^{1/2} \dots\dots\dots\dots\dots\dots\dots\dots\dots\dots(45)$$
$$u_* = \sqrt{gRS} \dots\dots\dots\dots\dots\dots\dots\dots\dots\dots\dots(46)$$
$$\tau = \rho u_*^2 = \mu\left(\frac{\partial u}{\partial z}\right) = \rho v\left(\frac{\partial u}{\partial z}\right) \quad \text{then } gRS \fallingdotseq v/T \text{ or } v \fallingdotseq \bar{U}RS\dots\dots\dots\dots(47)$$

Combining Eqs. (9)(11)and(12):

$$(1/n)R^{2/3}S^{1/2}/\sqrt{gRS} = 6.25 + 5.75\log(R/k_s)\dots\dots\dots\dots\dots\dots(48)$$

Combining Eqs. (10)(11)and(12):

$$(1/n)R^{2/3}S^{1/2}/\sqrt{gRS} = 4.25 + 5.75\log(n\sqrt{g}/SR^{1/6})\dots\dots\dots\dots\dots(49)$$
$$\text{From Eq.(14): } n = \sqrt{g}(6.25 + 5.75\log(R/k_s))/R^{1/6}\dots\dots\dots\dots(50)$$
$$\text{From Eq.(15): } n = \sqrt{g}(4.25 + 5.75\log(n\sqrt{g}/SR^{1/6}))/R^{1/6}\dots\dots\dots(51)$$
$$n \sim d_m^{1/6} \dots\dots\dots\dots\dots\dots\dots\dots\dots\dots\dots\dots(52)$$
$$[n] = [T/L^{1/3}]\dots\dots\dots\dots\dots\dots\dots\dots\dots\dots\dots\dots(53)$$

It is Dimensional and Varied with R from Eqs. (50) and (51), and by trial and error, it will approach to a constant while R is greater enough.

APPLICATION

Water budget balance, water scarcity, flood control, flood-sediment control, and landslide are such sensitive problems on our society and environment. Based the above theories, we need consider the corresponding application to reduce or solve those damages.

Runoff Curve Number (RCN) and Saturated Hydraulic Conductivity (Ksat) Estimation from the direct rainfall Measurements

Surface runoff can be estimated directly from conceptual models such as the runoff curve number (RCN) method or indirectly from physically based infiltration models such as the Green–Ampt method with. the key parameters involved in the runoff curve number (CN) and the saturated hydraulic conductivity (Ksat) respectively, which can be obtained from tables as functions of soil texture, management practice, and land use. The use of singular tabulated CN and Ksat values without verification can result in large errors in predicting surface runoff. Although the RCN method requires only the cumulative depth of rainfall at the end of the storm event (rainfall intensity, duration and distribution are not required), the use of Type II rainfall distribution (S curve) better mimics natural rainstorm events, which typically start with a low intensity, followed with a higher intensity, and end with a lower intensity. The curve number (CN) is an index representing the soil cover complex that reflects the response of a specific soil, under certain conditions (soil moisture and land cover), to a rainstorm event through runoff and infiltration. CN is a non-dimensional index having theoretically a value between 0 (no runoff) and 100 (no infiltration). For a specific soil cover condition, CN can be obtained from a range of rainfall depths and corresponding runoff depths by solving for S and I_a using the following CN equations as Eqs. (5) and (7).

The relationship between rainfall and runoff described by Eq. (5) requires the use of nonlinear regression analysis methods to obtain S and I_a values. Values of S and I_a were applied iteratively to Eq. (5) to produce a curve that best represents the measured data in Fig. 1. The solid line in Fig. 1 represents Eq. (5) using the optimal S and I_a values, whereas the dots represent the measured values. The intercept of the solid line with the x-axis gives .I_a. The CN value was obtained from Eq. (7).
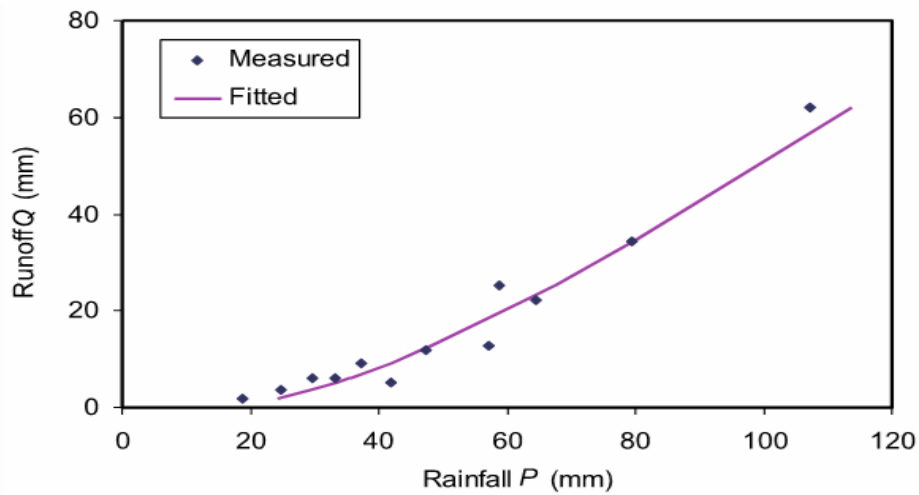
Fig. 1 Method of CN estimate from data obtained via the rainfall simulators measurements

When infiltration rate reaches a steady state condition (i.e. rates do not change with respect to time), this is defined in the literature as the saturated hydraulic conductivity, or Ksat. Ksat can be estimated from a range of data obtained via the rainfall simulators using the following mass balance equation:

$$f = p - q \quad \text{...} (54)$$

where: f = infiltration rate (mm/h), p = rainfall intensity (mm/h), and q = runoff rate (mm/h). In Eq. (54) the storage and evaporation are considered negligible and ignored due to the short duration of the rainfall experiments and relatively small size of the rainfall simulation plots. Ksat can be obtained from Eq.(54) by plotting f versus p in Fig. 2. This figure provides an example of the measured rainfall and infiltration values shown in dots, whereas the solid line represents the Ksat value for the given site. The figure indicates that the infiltration rate has reached a steady state condition through the rainfall simulator measurements, which corresponds to Ksat.

Higher soil moisture (M) conditions were also observed in fall than in summer. This was attributed to lower temperature and higher residue cover, which minimized evaporation from the soil surface. In summer, lower residue cover and higher temperature increased evaporation and evapotranspiration rates, thereby decreasing soil moisture. The initial abstraction I_a as a function of potential maximum retention S, and soil moisture content M.

We can regress the following equations as:

$$I_a = aS^b \quad \text{...}(55)$$

in two sets of a_1 and b_1 for summer while a_2 and b_2 for fall with $a_1 > a_2$ and $b_1 > b_2$.

$$I_a = cM^{-d} \dots\dots (56)$$

in two sets of c_1 and d_1 for summer while c_2 and d_2 for fall with $c_2 > c_1$ and $d_2 > d_1$.

$$CN = -eKsat + f \dots\dots (57)$$

in two sets of e_1 and f_1 for summer while e_2 and f_2 for fall with $e_2 > e_1$ and $f_2 > f_1$.

Initial abstraction I_a was not linearly proportional to potential maximum retention S (i.e. $I_a \neq 0.2S$) and increases with decrease of soil moisture M; and CN is interrelated with Ksat, showing an inversely proportional relationship between the two variables. However, a unique relationship does not exist as two curves were observed, based on seasonality.
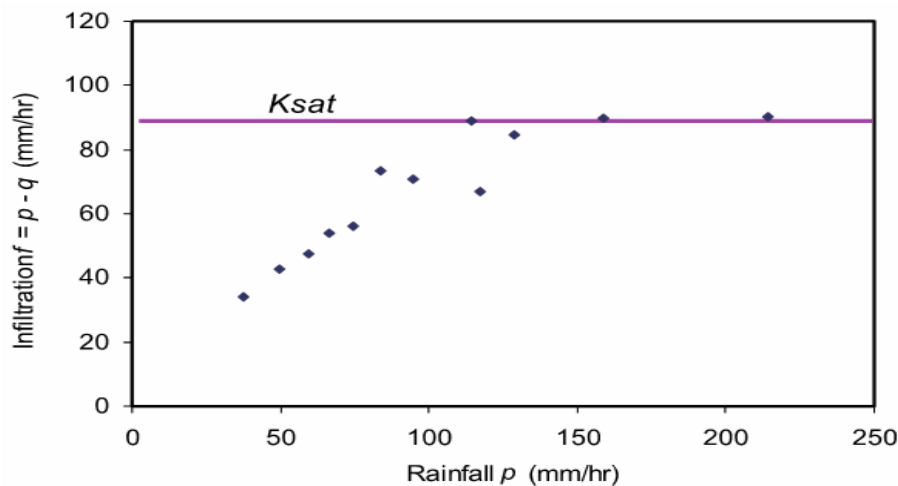
Fig. 2. Method of Ksat estimate from data obtained via the rainfall simulators

Estimations on Water Balance and Water Security

Water is one of the essential resources for all forms of life and it covers 71% of the Earth's surface. On Earth, 96.5% of the planet's water is found in oceans, 1.7% in groundwater, 1.7% in glaciers and the ice caps of Antarctica and Greenland, a small fraction in other large water bodies, and 0.001% in the air as vapor, clouds, and precipitation. Only 2.5% of the Earth's water is fresh water and 98.8% of that water is in ice and groundwater. Less than 0.3% of all freshwater is in rivers, lakes, and the atmosphere, and an even smaller amount of the Earth's freshwater (0.003%) is contained within biological bodies and manufactured products. Today, the competition for the fixed amount of water resources is much more intense, giving rise to the concept of peak water.

This very precious resource water is available over land surface through precipitation and it is the primary source for runoff generation over the land surface. In common course of

rainfall occurrence, a part of it is intercepted by the vegetation, buildings and other objects, lying over the land surface and prevent, to reach them on ground surface, called as interception. After satisfying the surface storage, infiltration and evaporation losses, excess rainfall moves over the land surfaces to reach the smaller rills is refer as overland flow. It involves building of greater storage over land surface and draining the same into channels or streams is termed as runoff.

Runoff forms a component of hydrologic cycle and is produced when the precipitation exceeds the evapo-transpiration, initial loss, infiltration and detention requirements of the land surface. Uncontrolled runoff leads to soil erosion posing serious threats to floods, environment, social and economic security in the country. To control soil erosion, it is essential to build up a strong base of water and land management and this can be achieved only through watershed development. Measurement and estimation of runoff is required for several purposes in hydrology such as to determine the priority water- sheds requiring catchment protection measures for soil and water conservation, to estimate ground water recharge after accounting for the runoff and the evaporation losses, for comparing the performance of alternate catchment protection measures to know the possibilities of flood hazards following rainfall events etc. estimation of runoff can be made by adopting simple or more elaborate estimation procedures which take into account the influence of the relevant watershed and rainfall parameters. One of the most important objectives of engineering hydrology is to calculate the water yield of the catchments to determine the flood flows for planning the discharge facilities of water storage structures. In situation where there is not sufficient and reliable data the calculation based on empirical methods lead to mistakes in determining the dimensions of water structures. A good runoff model includes spatially variable parameters such as rainfall, soil types and land use/land cover etc. Identification of runoff is also of critical importance where the basic reservoirs support drinking water needs of the population.

For utilization SCS-CN model, we need to know the factors influence CN, for examples, the land use (i.e. forested, residential, etc.), land treatment, hydrological condition, hydrological soil group, and antecedent soil moisture condition in the drainage basin.

Antecedent moisture is a term from the fields of hydrology and sewage collection that describes the relative wetness or dryness of a watershed. Rainfall/runoff relationship are well defined within the field of hydrology. It is the pervious runoff that is affected by antecedent moisture conditions, as runoff from impervious surfaces such as roads, sidewalks, and roofs will not be significantly affected by preceding moisture levels. For purposes of practical application three levels of AMC are recognized by SCS as follows:

AMC-I: Soils are dry but not to wilting point. Satisfactory cultivation has taken place.

AMC-Ⅱ: Average conditions.

AMC-Ⅲ: Sufficient rainfall has occurred within the immediate past five days. Saturated soil conditions prevail.

For conversion of CNI and CNIII into CNII from the field measurement data, the basic forms are shown as:

$$CNI = \alpha_1 CNII / (\beta_1 + \zeta_1 CNII) \quad\text{...(58)}$$

$$CNIII = \alpha_2 CNII / (\beta_2 + \zeta_2 CNII) \quad\text{.....................................(59)}$$

Where $\alpha_2 > \alpha_1$, $\zeta_2 > \zeta_1$, and $\beta_2 \fallingdotseq \beta_1$

.

$$\text{or } CNI = CNII - (\alpha_3 Y / (Y + \exp(\beta_3 + \zeta_3 Y))) \text{ with } Y = 100 - CNII \quad\text{............(58-1)}$$

$$\text{or } CNIII = CNII \exp(\zeta_4 Y) \quad\text{...(59-1)}$$

The estimated ground water utilization will help in water security planning for micro watershed, moreover runoff volume will help in design and construction of various soil and water conservation structures like spillways, drains, ponds, reservoirs etc. to assess the water yield of the watershed. From this it is also possible to determine its potential for different uses or purposes like irrigation, domestic use, power generation etc. On the other hand, the micro-watershed is presently facing problems of water scarcity thereby affecting the agricultural production of the area. Therefore, it is very essential to take up suitable measures for conservation of runoff generated in the area. If it is possible to harvest the maximum amount of runoff yield in the watershed, probably the water crisis in the area may be reduced.

To use water resources sustainably, it is important to understand the quantity of water resource spatially and temporally. The quality and quantity of water in natural systems are regulated by a complex set of processes such as the geochemical weathering reactions of minerals and human activities changing watershed characteristics, such as land cover, which in turn affect the biogeochemical processes that operate in the watershed. The SWAT (Arnold et al., 1998; Neitsch, Arnold, Kiniry, Williams, & King, 2002a, 2002b) was developed in the 1990s by the United States Department of Agriculture (USDA). It is a process based and spatially semi-dispersed hydrological and water quality model designed to calculate and route water, sediments, and nutrient from individual sub-watersheds all through the main stream watersheds towards its outlet. The SWAT model is an exceptionally flexible tool that has been used in numerous parts of the world to predict the effect of land-use management practices

on water, sediments and chemical yields from urban and farming activities in small to vast complex basins with different soils, land-use and management conditions, over a period of time (Eckhardt, Fohrer, & Frede, 2005). The SWAT model simulates the hydrological cycle according to Eq. (39) of water balance (Neitsch et al., 2005):

$$SW_t = SW_0 + \sum_{i=1}^{t} (R_{day} - Q_{surf} - E_a - W_{seep} - Q_{gw})$$ ....(60)

where, SWt is the final soil water content (mm), SWo is the initial soil water content in day i (mm), t is the time (days), Rday is the measure of precipitation in day i (mm), Qsurf is the measure of surface runoff in day i (mm), Ea is the amount of ET in day i (mm), Wseep is the measure of water entering the root zone from the soil profile on day i (mm), and Qgw is the measure of groundwater discharge in day i (mm). Water yield of a within a watershed is evaluated by the model based on Eq. (61):

$$W_{yld} = Q_{surf} + Q_{gw} + Q_{lat} - T_{loss}$$ ....(61)

Where Wyld is the measure of water yield (mm), Qsurf is the surface runoff (mm), Qlat is the lateral flow contribution to stream (mm), Qgw is the groundwater contribution to streamflow (mm), and Tloss is the transmission losses (mm) from tributary in the HRU by means of transmission through the bed. The estimation of surfacerunoff can be performed by the model using the SCS curve number system by the USDA Soil Conservation Service (Eqs. (5) and (7)). In Eq. (5), Qsurf is the accumulated runoff or rainfall excess (mm) and S is the retention parameter (mm).

$$Q_{lat} = 0.024 \frac{(2SSCsin\alpha)}{(\theta_d L)}$$ ....(62)

Where, Qlat = lateral flow (mm/day); S= drainable volume of soil water per unit area of saturated thickness (mm/day); SC=saturated hydraulic conductivity (mm/h); L=flow length, α =slope of the land, θd= drainable porosity and CN is the soil curve number.

The estimation of the base flow was done using Eq. (63):

$$Q_{gwj} = Q_{gwj-1}. \ e^{(-\alpha gw.\Delta t)} + W_{rchrg}. \ (1-e^{(-\alpha gw.\Delta t)})$$ ....(63)

Where Qgwj= groundwater flow into the main channel on day j; α gw =base flow recession constant; Δt= time step; and Wrchrg =the amount of recharge entering the aquifers (mm /day).

Observed data collected at a sampling site located were used for calibration and validation of the model. The configuration of the model involves the settings of the simulation period (start and finish date) and the selection of weather sources. In addition, selection of the

method for the estimation of surface run-off

(Curve Number or Green and Ampt method), channel water routing (variable or Muskingum method), and potential ET (Priestley, Penman-Monteith, and Hargreaves) is available in SWAT. The SWAT model estimated other important water balance components in addition to the monthly discharge of the watershed. Water yield is one of the important parameters estimated by the model for efficient water management and planning of the study area. The contribution made by each sub-watershed in the watershed area to the total water yield during the simulation period was examined using the calibrated model. To deal with water management issues, it is perfect to analyze and quantify the diverse components of hydrological processes occurring within the study area. The SWAT model estimated other pertinent water balance components in addition to the monthly flow or discharge. Reference Sathian and Syamala (2009), stated that the most imperative components of the water balance of a watershed are; precipitation, surface runoff, lateral flow, base flow, and ET

Estimation of Sediment Yield

For a gauged station, the sediment yield, $Q_s(t/ha)$ could be obtained from the discharge, Q (m^3/s), and concentration, C (mg/ liter), as:

$$Q_s = 0.0864CQ \dots\dots\dots\dots\dots\dots(64)$$

$$\text{or } Q_s = aQ^b \dots\dots\dots\dots\dots\dots(65)$$

and the sensitive factor will be the change of the land cover. From the SCS-CN model has the advantage for the ungauged area. Accurate estimation of runoff and sediment yield amount is not only an important task in physiographic but also important for proper watershed management. To proposes a seasonal relationship between Soil Conservation Services, runoff curve number (CN) and sediment yield (SY) will be very necessary.

The SCS-CN proportional equality (C = Sr) concept, it is possible to extend it for sediment yield as (Mishra et al. 2006):

$$C = S_r = DR \dots\dots\dots\dots\dots\dots(66)$$

Where, C is runoff coefficient, Sr is the degree of saturation and DR is the delivery ratio. In Eq. (66), all variables range from 0 to 1. Using the usual definition and $I_a = 0$, Eq. (66) can be expanded as:

$$C = \frac{Q}{P} = \frac{F}{S} = \frac{P}{P+S} = \frac{SY}{A} \dots\dots\dots\dots\dots\dots(67)$$

Eq. (46) implies that the sediment yield is directly proportional to the potential maximum erosion 'A' and runoff factor C is the proportionality constant. Alternatively,

$$SY = \frac{AP}{P + S}$$ ....(68)

For the given watershed characteristics or A and P, the actual sediment yield (SY) increases as S decreases, which is in conformity with the general notion that the higher the runoff amount, the higher will be the sediment erosion and its transport and hence higher the sediment yield and vice versa. As S→0 (or CN→100), SY→A since Q→P. Similarly, as S→∞(or CN→0), SY →0 since Q→0. It is consistent with the general notion that the surface runoff primarily drives sediment erosion. Thus, there appears to be a relation existing between SY and S, which can be described in power form as follows:

$$SY = \alpha (S)^{-\beta}$$ ....(69)

Where α and β are the coefficient and exponent, respectively. S and CN exists in an inverse relationship, Eq. (69) suggests SY to be high for the watersheds of low S, and vice versa. The following text endeavors to support this logic.

To develop the concept following Mishra and Singh (2003a, b), the Horton's method (Horton 1932) can be expressed mathematically as:

$$\frac{F}{S} = (1 - e^{-\alpha t})$$ ....(70)

An assumption of rainfall P growing linearity with time t, which is a valid and reasonable assumption for infiltration rate computation in experimental tests (Mishra and Singh 2004a, b),

$$\frac{P}{S} = \alpha t$$ ....(71)

Referring to Eq. (3),

$$S_t = S_0 - F$$ ....(72)

where, St is the available storage for water retention in a soil column at time t, So is the potential storage space available for moisture retention in the soil column. Parameter So is shown to be equivalent to the potential maximum retention of the SCS-CN model (S = So).

Coping Eq. (72) into Eq. (70) (for S = So) yields:

$$S = S_t(1 + \alpha t)$$ ....(73)

Eq. (73) shows the variation of S with rain duration (t). It shows that as the potential maximum retention increases, the rain duration increases and vice versa.

Novotny and Olem (1994) showed a power relationship between C and DR:

$$DR = \alpha C^\beta$$ ....(74)

DR is a dimensionless ratio of the sediment yield (SY) to the total potential erosion (A) in the contributing Watershed:

$$DR = \frac{SY}{A}$$ ....(75)

The coefficient C is also dimensionless and expressed in terms of Q and P as:

$$C = \frac{Q}{P} = \frac{F}{S} = \frac{P}{P+S}$$ ....(76)

Coupling Eq. (74) with Eq. (75) and Eq.(76), C = P/(P+S) yields

$$\frac{SY}{A} = \alpha \left[\frac{P}{P+S} \right]^{\beta}$$ ....(77)

For the above application, the land-use, land management, the hydrological condition, such as rainfall intensity on the seasonal varieties are all sensitive factors. We can regress the relationship between SY and S for different seasons as forms:

$$SY = \alpha_i S^{-\beta_i}$$ ....(78)

Time of Concentration (TC),and Lag Time (TL)

Time of concentration (Tc) is the time required for runoff to travel from the hydraulically most distant point in the watershed to the outlet. The hydraulically most distant point is the point with the longest travel time to the watershed outlet, and not necessarily the point with the longest flow distance to the outlet. Time of concentration is generally applied only to surface runoff and may be computed using many different methods. Time of concentration will vary depending upon slope and character of the watershed and the flow path. In hydrograph analysis, time of concentration is the time from the end of excess rainfall to the point on the falling limb of the dimensionless unit hydrograph (point of inflection) where the recession curve begins
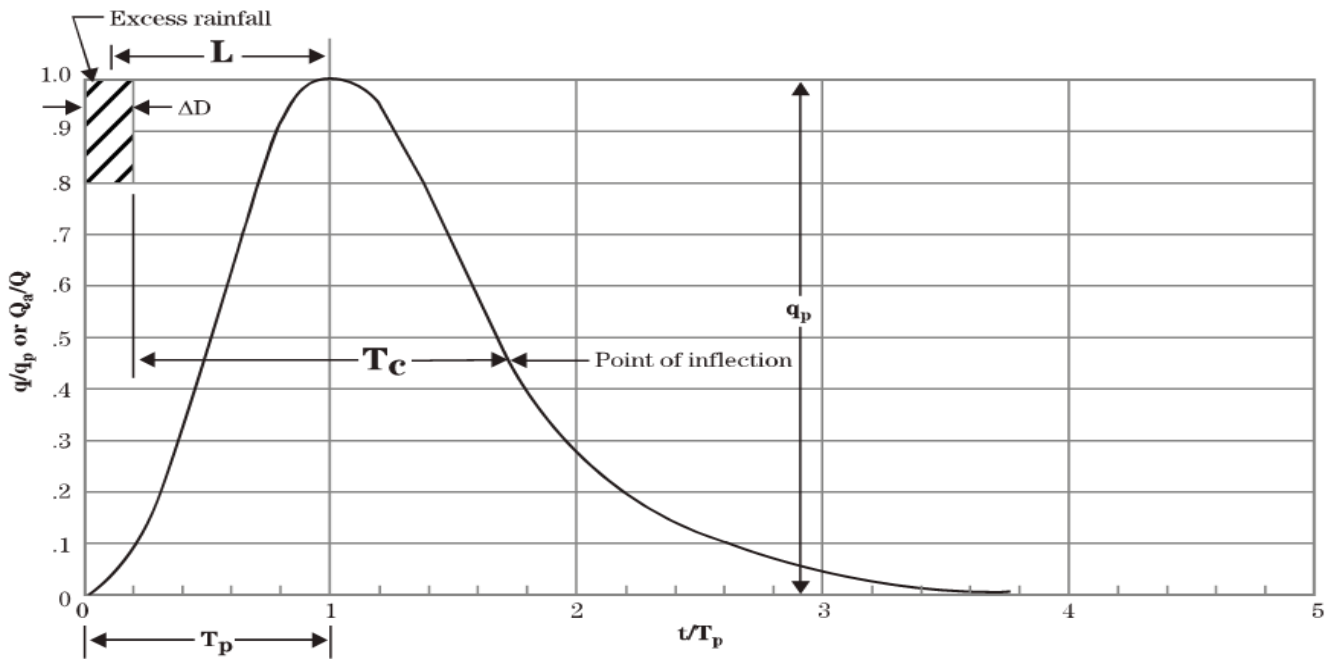
Fig. 3. The relation of time of concentration (TC) and lag (TL) to the dimensionless unit hydrograph

Various researchers found that for average natural watershed conditions and an approximately uniform distribution of runoff:

$$TL=0.6TC \dots\dots\dots\dots\dots\dots\dots\dots\dots\dots\dots\dots\dots\dots\dots\dots\dots\dots\dots\dots(79)$$

where: TL = time lag, (hr) and Tc = time of concentration, (hr) USDA(2010) present the SCS method for watershed of time of concentration and time lag and velocity versus slope for shallow concentrated flow on Hydrology National Engineering Handbook (No.630) Ockert J. Gericke and Jeff C. Smithers (2014) reviewed the methods used to estimate catchment response time for the purpose of peak discharge estimation and said Large errors in peak discharge estimates at catchment scales can be ascribed to errors in the estimation of catchment response time. The time parameters most frequently used to express catchment response time are the time of concentration (TC), lag time (TL) and time to peak (TP). The TC is recognized as the most frequently used time parameter, followed by TL. In acknowledging this, as well as the basic assumptions of the approximations TL = 0.6TC and TC ≈ TP, along with the similarity between the definitions of the TP and the conceptual TC, it was evident that the latter two time parameters should be further investigated to develop an alternative approach to estimate representative response times that result in improved estimates of peak discharge at these catchment scales.

He announced that Time variables can be estimated from the spatial and temporal distributions of rainfall hyetographs and total runoff hydrographs. To estimate these time variables, hydrograph analyses based on the separation of: (a) total runoff hydrographs into direct runoff and baseflow; (b) rainfall hyetographs into initial abstraction, losses and effective rainfall; and (c) the identification of the rainfall−runoff transfer function are required. A convolution process is used to transform the effective rainfall into direct runoff through a synthetic transfer function based on the principle of linear super-positioning, e.g. multiplication, translation and addition. Effective rainfall hyetographs can be estimated from rainfall hyetographs in one of two different ways, depending on whether observed streamflow data are available or not. In cases where both observed rainfall and streamflow data are available, index methods such as: (i) the Phi-index method,where the index equals the average rainfall intensity above which the effective rainfall volume equals the direct runoff volume, and (ii) the constant-percentage method, where losses are proportional to the rainfall intensity and the effective rainfall volume equals the direct runoff volume, can be used. However, in ungauged catchments, the separation of rainfall losses must be based on infiltration methods, which account for infiltration and other losses separately. The SCS runoff curve number method is internationally the most widely used. In general, time variables obtained from hyetographs include the peak rainfall intensity, the centroid of effective rainfall and the end time of the rainfall event. Hydrograph-based time variables generally include peak discharges of observed surface runoff, the centroid of direct runoff and the inflection point on the recession limb of a hydrograph.

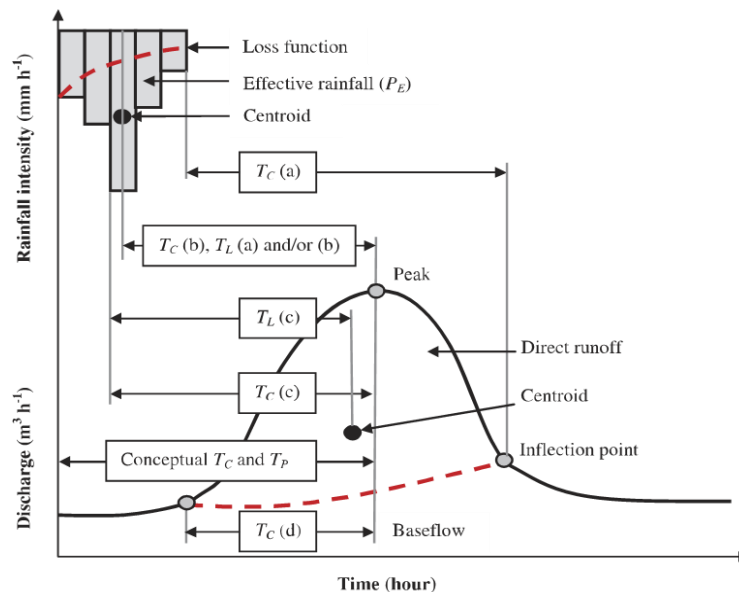He schemed the following figure to explain:

Fig. 4. Schematic diagram illustrative of the different time parameter definitions and relationships

The SCS-CN system expresses the following formula on TC and TL:

$$T_{C2} = \frac{L_O{}^{0.8}\left[\frac{25\,400}{CN} - 228.6\right]^{0.7}}{706\,9\,S^{0.5}}$$ ....(80)

where TC2 is overland time of concentration (min), CN is the runoff curve number, LO is length of overland flow path (m), and S is average catchment slope (m/m).

$$T_{L2} = \frac{L_H{}^{0.8}\left[\frac{25\,400}{CN} - 228.6\right]^{0.7}}{281.42\,S^{0.5}}$$ ....(81)

where TL2 is lag time (h), CN is the runoff curve number, LH is the hydraulic length of the catchment (km), and S is the average catchment slope (m/m).

Dagnenet Sultan, et al,(2022) studied Lag time (TL) and time of concentration (TC) are two measures of how quickly a stream responds to runoff-producing rainfall. These parameters are the main inputs used to estimate peak flow under flood conditions in ungauged watersheds. Many empirical methods have been proposed to estimate TL and TC, but the validity of none of them has been tested. This study compared 10 commonly used methods by using measured TL and TC. Measured median values of TL and TC for 176 rainfall–runoff events were used to evaluate the performance of empirical methods. For individual watersheds, the estimates of TL and TC differed by up to 2.6 h and 4.4 h, respectively. Most of the empirical methods tended to substantially underestimate TL and TC, which would lead to overestimation of runoff volume. The collection of formula for TC and TL will be very applicable for us.

Most of the published methods for empirical measurement of TL and TC are based on data gathered from a particular geographic region with specific physical attributes and rainfall patterns. Majority of methods were developed from watersheds of temperate climate of the United States where rainfall runoff mechanisms differ considerably than tropical regions. He concluded that we compared the performance of 10 of these methods in six small agricultural watersheds in tropical Ethiopia. Majority of methods were developed from watersheds of temperate climate of the United States where rainfall runoff mechanisms differ considerably than tropical regions. Our study was based on high-frequency hydrometric observations in the six watersheds for five consecutive rainy seasons (2014–2019). Our results show that values of TL and TC determined for a particular watershed by the various methods varied considerably (up to 2.65 h and 4.45 h for TL and TC, respectively) and without systematic differences according to the method used.

Our statistical analysis of the performance of the 10 methods showed most of them to have positive or negative statistical biases of at least 25%. However, TL and TC estimated by

the SCS velocity methods were closest to the measured values, likely because both methods take into consideration the mixed (overland and channel) flow that is characteristic of tropical regions. Six of the selected methods greatly underestimated TL and TC and, if they were applied in tropical regions, could lead to over-estimations of peak flow, construction of unnecessarily large hydraulic infrastructure, and excessively conservative estimations of flood height, thus incurring unnecessary material and construction costs for projects. The local characteristics of the watersheds (soil type, topography, conservation practices, land cover, soil moisture, and climate) affected the estimates of TL and TC, which demonstrates the need for caution in the selection of empirical methods for application outside the region in which they were developed. The contributions of his work are abstracted as following (Table 1 and Figs. 5 and 6):

DISCUSSION AND CONCLUSSIONS

Risk Assessment on Landslides Hazards

Landslides are natural geologic processes that cause different types of damage and affect people, organizations, industries, and the environment. Globally, landslides cause billions of dollars in damage and thousands of deaths and injuries each year. Human activities, such as deforestation and urban expansion, accelerate the process of landslides.

Landslide hazard models have been developed in various ways and include: a) landslide inventory, b) statistical modeling, c) heuristic methods, d) process-based modeling, and e) probabilistic or stochastic modeling, and f) a physically-based model based on a combination of the infinite slope equation of the Mohr-Coulomb failure law and a hydrological component based on steady-state shallow subsurface flow.

Uncertainties are usually introduced by soil-related parameters that have different properties and vary over space in different ways. The soil spatial variation captured in a soil map is often generalized because of many uncertainties involved in soil mapping. Soil variation is more continuous than discrete and therefore an approach that models the soil as a continuum is more appropriate.

Modeling uncertainty may be handled through probability theory or fuzzy set theory. Probability theory uses probabilistic models to quantify the uncertainty associated with the prediction of the phenomenon, and measures incomplete knowledge through objective modeling. Fuzzy set theory, on the other hand, models uncertainty based on expert knowledge, and measures incomplete knowledge through subjective modeling. Therefore, methods of fuzzy classification may be used to account for uncertainty and replace crisp classification

methods by providing class overlap that is more realistic for modeling continuous landscape patterns. Other methods, such as Bayes theorem, provide a potential means of converting knowledge of predictive correlations from a fuzzy classification of landforms in combination with landslide location data, to landslide hazard probabilities. Bayes theorem has been applied for geologic hazard prediction, geologic soil-landscape modeling, and more recently in environmental science or wildlife studies.

Multi-risk assessment is becoming a valuable tool for land planning, emergency management and the deployment of mitigation strategies. Multi-risk maps combine all available information about hazard, vulnerability, and exposed values related to different dangerous phenomena, and provide a quantitative support to complex decision making. The different indicators, physical risk, hydrogeological risk and aggravating factor by applying appropriate weights based on expert knowledge were suggested. Case by case, the most convenient weighting strategies, such as Budgetary Allocation, Fuzzy Sets, and Analytic Hierarchy Process were considered. Sensitivity analysis for each indicator or factor must be done for the information of the influence for each factor on the results and purpose of uncertainty test on promotions of the more efficient choice on the factors when we calculate the risk. Combining risks with different characteristics, metrics and distributions is extremely difficult, but it is useful for some public administrations, which have to manage and plan mitigation strategies not only on critical situations deriving from a single specific risk, but on the territory in its complexity considering the interaction between threats, processes, and dynamics.

Table 1

Empirical methods used in watersheds with various flow regimes in different climatic regions around the world to estimate lag time and time of concentration.

| Method name	Equation	Dominant flow regime	Description	References
USBR	$T_C = \tau\left(\dfrac{0.87 \times L_{CH}^2}{1000 S_{CH}}\right)^{0.385}$	Channel flow	Developed in the USA and used especially for culvert design based on California Culvert Practice (CCP, 1955; cited by Gericke et al., 2016). T_C is time of concentration (h), L_{CH} is length of the longest watercourse (km), S_{CH} is average main watercourse slope (m m^{-1}), and τ is a correction factor ($\tau = 2 - 0.5 \log^A$, where A is watershed area (km^2).	United States Bureau of Reclamation (USBR) (1973)
Snyder	$T_L = C_t(L \times L_C)^{0.3}$	Overland flow	A synthetic unit hydrograph (SUH) method derived from the relationships between standard unit hydrographs and geomorphological watershed descriptors from 20 basins with watershed areas from 25 to 25,000 km^2 in the Appalachian Highland, USA. T_L is lag time (h), C_t is catchment storage coefficient or lag factor (typically 1.35–1.65) and is dependent on basin properties (slope and storage), L is main channel length (km), and L_C is centroid distance (km).	Snyder (1938)
SCS Lag	$T_L = \dfrac{(L_{CH}^{0.8} \times (Snat + 1)^{0.7})}{1900 \times S^{0.5}}$	Overland flow	Model developed for 24 small rural basins ($A < 8$ km^2) in the USA, where T_L is lag time (h); L_{CH} is length of longest watercourse (feet); S_{nat} is potential maximum storage after commencement of runoff (inch). $S_{nat} = 1000/CN{-}10$, S is average watershed slope (%), and CN is weighted curve number.	SCS (1972, 1985); Li and Chibber (2008)
FAA	$T_C = 1.8 \times (1.1 - C)L^{0.5}S^{0.34}$	Overland flow	Developed from airfield drainage data of a small watershed by the US Corps of Engineers. T_C is time of concentration (h); L is main flow length (feet); S is average slope of flow path (%); and C is a rational method coefficient	Federal Aviation Authority (FAA) (1970); McCuen et al. (1984)
Bransby Williams	$T_C = 0.605 * \dfrac{L}{(100 S_o)^{0.2} A^{0.1}}$	Channel flow	Originally developed in tropical East India; limited to rural watersheds of < 130 km^2 area. T_C is time of concentration (h), A is watershed area (km^2), L is main channel length (km), S_o is main channel average slope (m/m), average gradient (ratio between average gradient and length L of water course).	Williams (1922); Li and Chibber (2008)
Kirpich	$T_C = 0.0663 L^{0.77} S_o^{-0.385}$	Channel flow	Developed for small drainage basins using data from six small basins in Tennessee, USA, with basin areas of 0.0051–0.433 km^2 and slopes of 3–12%. T_C is time of concentration (h), L is main channel length (km), and S_o is main channel slope (m/m).	Kirpich (1940); Li and Chibber (2008)
Carter	$T_C = 0.0977 \dfrac{L^{0.6}}{S^{0.2}}$	Channel flow	Developed for natural channels in the USA ($A < 20.72$ km^2). T_C is time of concentration (h), L is the main channel length (km), and S is channel slope (m/m).	Carter (1961)
Ventura	$T_C = 4A^{0.5}L^{0.5}H^{-0.5}$	Channel flow	Developed using data of rural basins in the Po Valley, Italy, used for natural channels. T_C is time of concentration (h), A is watershed area (km^2), H is height difference between edges of main water line (m); and L is main channel length (km).	De Almeida et al. (2014); Kaufmann de Almeida et al. (2017); Salimi et al. (2017)
Simas–Hawkins	$T_L = 53.14 \times W^{0.594} S^{-0.150} \times S_{nat}^{0.313}$	Mixed flow	Developed using data from 168 watersheds ($A = 0.0012$–14 km^2) from > 50,000 rainfall–runoff events in the USA. T_L is lag time (h), S is average watershed slope (m/m), S_{nat} is storage coefficient (in) used in the Curve Number (CN) method, W is width (ft) of the watershed, which is the ratio of watershed area (acres) to the longest flow path (L_{CH}).	Simas and Hawkins (1996)
SCS Velocity	$T_C = T_{sheet} + T_{shallow\ concentrated} + T_{open\ channel}$. i.e. $T_C = \dfrac{5.48(n_0 L_S)^{0.8}}{(P_2)^{0.5}(S)^{0.4}} + \dfrac{L_{SC}}{60V} + \dfrac{nL_{OC}}{60R^{0.67}S_o^{0.5}}$	Mixed flow	Developed by US Soil Conservation Service. T_C is time of concentration (min), which is the sum of travel times for sheet flow (T_{sheet}), shallow concentrated flow ($T_{shallow\ concentrated}$), and open channel flow ($T_{open\ channel}$). n_0 is Manning's roughness coefficient for sheet flow; L_S is sheet flow path length (m); P_2 is the 2-year return period, 24 h rainfall depth (mm); S is slope of the land surface (m/m); V is shallow concentrated flow velocity (m/s), which is obtained as a function of surface slope ($V = 4.9178\sqrt{S}$ [NRCS, 1986]); L_{OC} is channel flow length (m); L_{OC} is channel bottom slope (m/m); n is Manning's roughness coefficient for open channel flow; S_o is channel bottom slope (m/m); and R is hydraulic radius (m).	SCS Velocity (1986); NRCS TR-55 (2010)
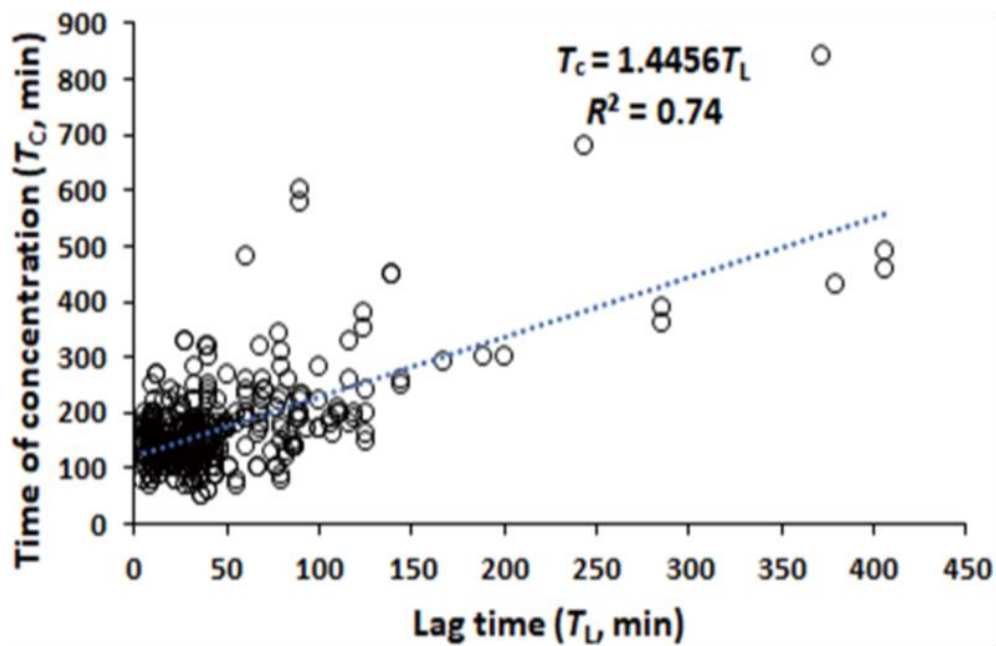
Fig. 5. Lag time versus time of concentration for 186 rainfall–runoff events in the six watersheds of this study.

Risk assessment for spatial prediction of landslide hazard, especially for geophysical hazards like landslides, depends on probability estimation of frequency, magnitude of future events, and their adverse consequences. Urban settlements in flat areas are generally not affected by landslide hazards but settlements in hilly areas or near to hilly areas are often affected by these hazards. Risk is defined as a function of both hazard and vulnerability. Landslide risk is expressed as a probability that an area will undergo substantial levels of damage from a landslide event. To assess the risk of landslide hazard in an area, the topography is visualized in a digital environment and their extraction through several existed procedures is important. Being an important source of information for many other applications in identifications of topographic settings susceptible to land sliding.

Future Studies of on the Application of SCS-CN with Seasons and Spatial Variations

The sensitivity analyses on the application of the SCS-CN are needed to study, especially watershed runoff to meteorological parameters, the Manning overland roughness coefficient values, the overland concentration time, he velocity of overland flow on Manning equation, and hydro-morphodynamic parameters, such as the soil type, including moisture, soil porosity, groundwater, and the hydrological factors, such as evaporation, transpiration, etc. both on spatial and seasonal changes.
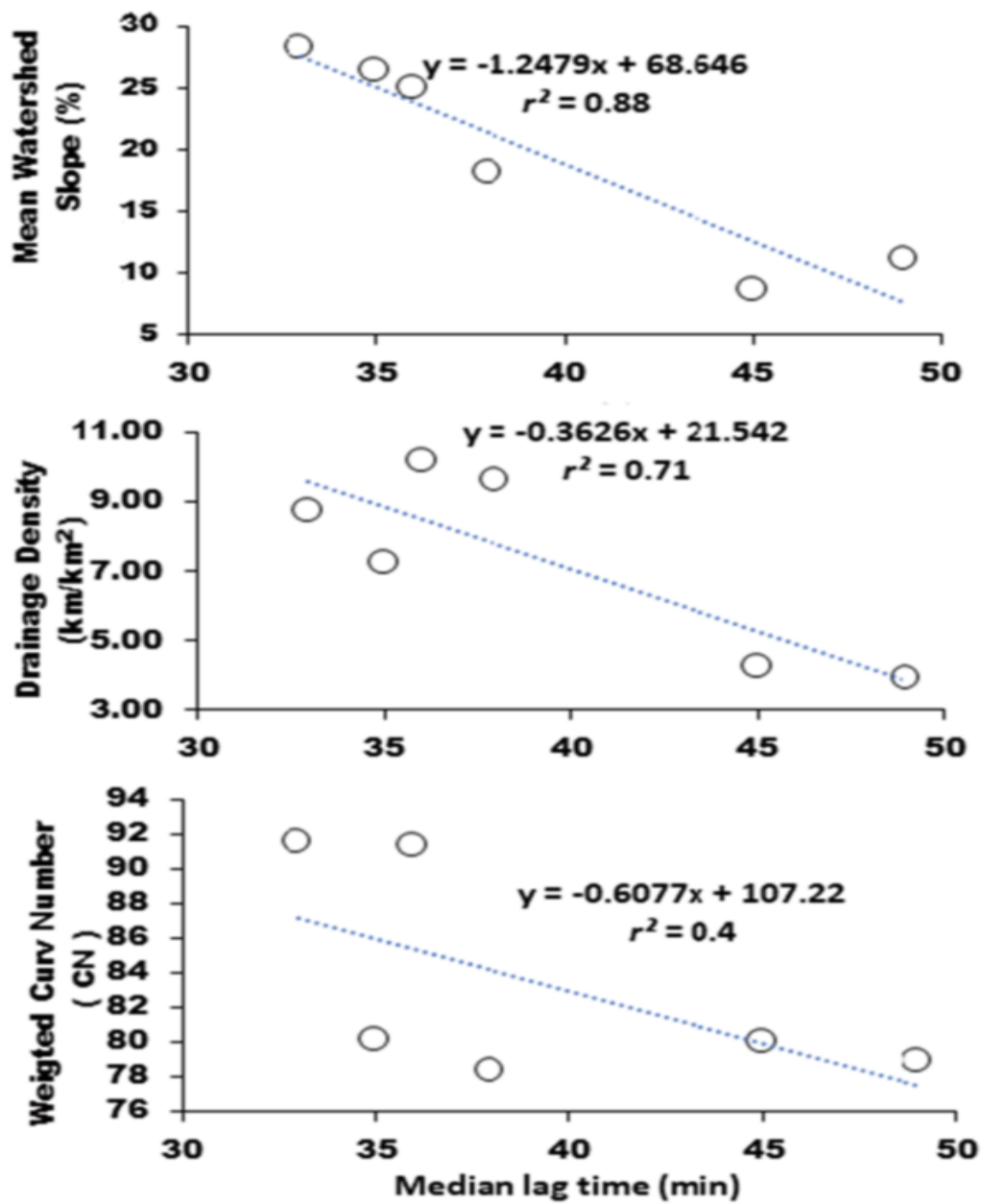
Fig. 6. Measured median lag time versus mean watershed slope, drainage density, and weighted curve number for each of the six watersheds of this study.

REFERENCES

Allen RG, Pereira LS, Raes D, Smith M (1998) Crop evapotranspiration guidelines for computing crop water requirements, FAO Irrigation and drainage paper No. 56, Food and Agriculture Organization of the United Nations FAO, Rome

Arnold J.G., Srinivasan R., Muttiah R.S. and Williams J.R. (1998). Large area hydrologic modeling and assessment Part 1: Model development. Journal of the American Water Resources Association, 34(1), 73-89.

Bray, D.I. (1979). "Estimating Average Velocity in Gravel bed Rivers." Journal Hydraulic Division, ASCE, 105(HY9), 1103–1122

Brocca, L., Melone, F., Moramarco, T., Wagner, W., Naeimi, V.,Bartalis, Z., and Hasenauer, S.(2010): Improving runoff predictionthrough the assimilation of the ASCAT soil moisture product, Hydrol. Earth Syst. Sci., 14, 1881–1893, doi:10.5194/hess-14-1881-2010.

Brocca, L., Moramarco, T., Melone, F., Wagner, W., Hasenauer, S., and Hahn, S.(2012): Assimilation of surface and root-zone ASCAT soil moisture products into rainfall-runoff modelling, IEEE T. Geosci. Remote, 50, 2542–2555.

Brooks, R. H. and Corey A. T.(1964): Hydraulic properties of porous media, Hydrol. Pap. 3, Colorado State Univ., Fort Collins, USA.

Bruschin, J. (1985). "Discussion on Brownlie (1983): Flow Depth in Sand-bed Channels." Journal of Hydraulic Engineering, ASCE, 111, 736–739.

Carter RW., 1961. Magnitude and frequency of floods in suburban areas. US Geological Survey Professional Paper, 424:9–11.

Chow, V.T. (1959). Open Channel Hydraulics. Mc-Graw Hill, Singapore.

ERA (Ethiopian Road Authority) Design manual, 2013.

Green, W. H. and Ampt, G. (1911): Studies of soil physics, part I – the flow of air and water through soils, J. Agr. Sci., 4, 1–24.

Horton RE (1932) Drainage basin characteristics. EOS Trans AGU 13:350–361

Limerinos, J. T. (1970). Determination of the Manning Coefficient for Measured Bed Roughness in Natural Channels. Water Supply paper 1898-B, U.S. Geological Survey, Washington D.C.

Ma, Y. L-THIA: A Useful Hydrologic Impact Assessment Model. Nature and Science. 2004. 2 (1) 68-73

Manfreda, S., Lacava, T., Onorati, B., Pergola, N., Di Leo, M., Margiotta, M. R., and Tramutoli, V.(2011): On the use of AMSU-based products for the description of soil water content at basin scale, Hydrol. Earth Syst. Sci., 15, 2839–2852, doi:10.5194/hess-15- 2839-2011.

Matgen, P., Heitz, S., Hasenauer, S., Hissler, C., Brocca, L., Hoffmann, L., Wagner, W., and Savenije, H. H. G.(2012a): On the potential of METOP ASCAT-derived soil wetness indices as a new aperture for hydrological monitoring and prediction: a field evaluation over Luxembourg, Hydrol. Process., 26, 2346–2359.

McCuen R.H. (2003). Hydrologic Analysis and Design. 3rd edn., Prentice Hall, New Jersey.

Meyer-Peter, E. and Muller, R. (1948). Formulas for Bed-load Transport. Proceed. Third Meeting of IAHR, Stockholm, Sweden, 39–64.

Microsoft Corporation, 2018. Microsoft Excel. Retrieved from https://office.microsoft.com/excel〉.

Mishra S.K. and Singh V.P. (2003). Soil conservation service curve number (SCS-CN) methodology. Kluwer Academic, Dordrecht, The Netherlands.

Mishra SK, Singh VP (2003a) SCS-CN method Part-II: analytical treatment. Acta Geophysica Polonica 51(1):107–123

Mishra SK, Singh VP (2003b) Soil conservation Service Curve Number (SCS-CN) Methodology. Kluwer Academic Publishers, Dordrecht

Mishra SK, Singh VP (2004a) Validity and extension of the SCS-CN method for computing infiltration and rainfall-excess rates. Hydrol Process 18(17):3323–3345

Mishra SK, Singh VP (2004b) Long-term hydrologic simulation based on the Soil Conservation Service curve number. Hydrol Process 18:1291–1313

Mishra SK, Tyagi JV, Singh VP, Singh R (2006) SCS-CN-based modeling of sediment yield. J Hydrol 324:301–322

Novotny V, Olem H (1994) Water quality: prevention, identification, and management of diffuse pollution . Wiley, NY

NRCS (Natural Resource Conservation Service), 1986. Urban hydrology for small watersheds TR-55. USDA Natural Resource Conservation Service, Conservation Engineering Division Technical Release 55, 164. Technical Release 55.

Ockert J. Gericke & Jeff C. Smithers (2014) Review of methods used to estimate catchment response time for the purpose of peak discharge estimation. Hydrological Sciences Journal, ISSN: 0262-6667 (Print) 2150-3435 (Online) Journal homepage: https://www.tandfonline.com/loi/thsj20

Ponce V.M. (1989). Engineering Hydrology, Principles and Practices. Prentice Hall, Englewood Cliffs, NJ Ponce, V.M., and Hawkins, R.H. Runoff Curve Number: Has It Reached Maturity? Journal of Hydrologic Engineering. 1996. 1 (1) 11-19.

Schulze, R.E., Schmidt, E.J., Smithers, J.C., 1992, PC Based SCS Design Flood Estimates for Small Catchments in Southern Africa, SCS-SA User Manual: Pietermaritzburg, South Africa, University of Kwa-Zulu-Natal, Department of Agricultural Engineering, Report No. 40.

Rawls, W. J., Ahuja, L. R., Brakensiak, D. L., and Shirmohammadi, (1993). A.: Infiltration and soil water movement, in: Handbook of Hydrology, edited by: Maidment, D. R., 5.1–5.51.

Rossman L.A., Dickinson R.E., Schade T., Chan C., Burgess E.H., Sullivan D. and Lai D.(2003). SWMM5 - the Next Generation of EPA's Storm Water Management Model.Ch. 16 in Innovative Modeling of Urban Water Systems Monograph 12. Proc of the 2002 Conference on Stormwater and Urban Water Systems Modeling, Feb 20-21, Toronto, Ontario, Canada, pp. 339-356.

Sathian, K. K., Syamala, P. (2009). Application of GIS integrated SWAT model for basin level water balance.〈(http://www.csre.iitb.ac.in/csre/conf/wpcontent/uploads/fullpapers/OS5/0S5_15.pdf〉, accessed 8/2016).

Sharpley A.N. and Williams J.R. (1990). EPIC-Erosion/productivity impact calculator-1:model documentation. USDA-Technical Bulletin No. 1768, US Government Printing Office, Washington DCSoil Conservation Service (SCS), 1972, National Engineering

Handbook, Section 4, Hydrology: Washington DC, United States Department of Agriculture

Strickler, A. (1923). Beitrage zur frage der geschwindig-keitsformel und der rauhigkeitszahlen fuer stroeme kanaele und geschlossene leitungen. Mitteilungen des eidgenossischen Amtes fuer Wasserwirtschaft 16. Bern, Switzerl

Thomas, A. (2001): A Geographic Information System Methodology for Modelling Urban Groundwater Recharge and Pollution. PhD Thesis. The School of Earth Sciences. The University of Birmingham, Birmingham, United Kingdom. September 2001.

United States Department of Agriculture (USDA), 1986, Urban Hydrology for Small Watersheds: Springfield, VA, United States Department of Agriculture, Natural Resources Conservation Services, Conservation Engineering Division, Technical Release TR-55, 164 p.

USDR (1973), Design of Small Dam 2ed edition, Water Resources Technical Publication, Washington DC.

USDA-SCS, 1993: National Engineering Handbook. Section 4, Hydrology. United States Department of Agriculture, Soil Conservation Service. Washington, DC.

http://www.nrcs.usda.gov/wps/portal/nrcs/detailfull/national/water/?cid=stelprdb1043063 (Accessed on 18 June 2014)

Wait, I.W., & Simonton, D.S., 2015. Evaluation of the SCS lag time method for steep, in: Rural Watersheds In World Environmental and Water Resources Congress, pp. 2558–2567.